Gust-front factor: A new framework for the analysis of wind load effects in gust-fronts

Dae Kun Kwon[a], Ahsan Kareem[a]

[a] NatHaz Modeling Laboratory, University of Notre Dame, USA

ABSTRACT: In comparison with atmospheric boundary-layer winds, which are customarily treated as stationary, gust-front winds such as a thunderstorm/downburst exhibit strong nonstationarity. In storms characterized by a gust-front, wind speed changes rapidly during a short time period. In order to realistically describe attendant loads effects, a new analysis framework is presented which is named the gust-front factor (G_{G-F}) approach. The gust-front factor, akin to the gust loading factor in boundary-layer winds which has world-wide acceptance in codes and standards, is introduced and can be utilized in conjunction with the existing design standards. The G_{G-F} based approach encapsulates both static and dynamic characteristics of gust-front wind effects on structures through the following features that distinguish them from conventional boundary-layer flows: variation in the vertical velocity profile; dynamic effects induced by the sudden rise in wind speed; non-stationarity of turbulence in gust-front wind; transient aerodynamics.

KEYWORDS: Gust-front factor, Gust-front, thunderstorm/downburst, nonstationarity

1 INTRODUCTION

Due to spatio-temporal fluctuations in boundary-layer winds, dynamic effects of wind on structures exposed to these conditions have been of major concern in structural engineering. To account for the gustiness of the turbulent boundary-layer wind on structures, most international codes and standards have adopted the concept of a gust loading factor which was first introduced by Davenport[1] and more recently recast into a new format by Kareem and Zhou[2]. In comparison with boundary-layer winds that have generally been regarded as stationary, gust-front winds such as in thunderstorm(s)/downburst(s) exhibit distinct nonstationarity, i.e., rapid changes in wind speed during short time intervals. The significance of these transient wind events and their load effects can be readily surmised from the analysis of thunderstorm databases both in the U.S. and around the world, which suggest that indeed these winds actually represent the design wind speed for many locations.

The mechanics of gusts associated with convective gust-fronts differs significantly from conventional turbulence both in its kinematics and dynamics. The key distinguishing attributes are the contrasting velocity profile with height and the statistical nature of the wind field. In gust-fronts, the traditional velocity profile does not exist; rather it bears an inverted velocity profile with maxima near the ground potentially exposing low- to mid-rise structures to higher wind loads. Furthermore, such a change in the approach flow profile/kinematics, even in a steady state flow, would introduce a major change in the flow-structure interaction that may differ significantly from the corresponding boundary-layer flow case. This is compounded by the inherent transient nature of energetic convective gusts that rapidly increase in amplitude and direction raising serious questions regarding the applicability of conventional aerodynamic loading theories. The nonstationarity features are the critical issues in these wind events, which are being examined utilizing full-scale measurements, e.g., Wang & Kareem[3] and Chen & Letchford[4].

Thus, design loads in gust-front wind obtained from conventional analysis frameworks in codes and standards such as the gust loading factor approach (ASCE 7[5]) may not be appropriate and it calls for a careful examination of traditional design procedures. In an effort to establish a new procedure in this type of wind load effect on structures, this study introduces a gust-front factor based approach that accounts for the changes in load effects in gust-front winds. The gust-front factor, akin to the gust loading factor in boundary-layer winds widely accepted in codes and standards, is designed to be used in conjunction with the existing design standards, ASCE 7 (Kareem et al.[6]).

2 MODEL OF GUST-FRONT WINDS

In this study, analytical/empirical models of downburst winds that characterize their spatio-temporal features are employed. For convenience, it is generally assumed that gust-front winds at any time and height may be factorized in terms of the product of a vertical profile and a time function, e.g.,

$$V_{G-F}(z,t) = V_{G-F}(z) \cdot V_{G-F}(t) \qquad (1)$$

where, subscript G-F : abbreviation for gust-front wind, $V_{G-F}(z)$: vertical profile of gust-front wind, $V_{G-F}(t)$: normalized time function of gust-front wind.

2.1 Vertical profile, $V_{G-F}(z)$

The description of the vertical profile of gust-front winds is critical in evaluating the wind effects on structures, however, there is very limited full-scale data along the height available to reliably identify the vertical profile. Several analytical/empirical models of downburst have been proposed by several researchers (e.g., Vicroy[7]) to describe the vertical profile of gust-front winds. It has been reported that in gust-fronts, the traditional velocity profile does not exist; rather it bears an inverted velocity profile with maxima near the ground. This study with loss of generality utilizes the model proposed in Vicroy[6] which is expressed by

$$V_{G-F}(z) = A \cdot V_{max} \left[e^{b_1(z/z_{max})} - e^{b_2(z/z_{max})} \right] \qquad (2)$$

where, V_{max} : maximum horizontal wind speed, z_{max} : a height where V_{max} occurs, A : constant can be determined from model constants b_1 and b_2.

2.2 Time function, $V_{G-F}(t)$

The time function describes the time-varying mean of wind speeds in nonstationary wind. One can derive models based on actual measurements, e.g., the Andrews AFB downburst which has been well-documented and has been utilized to examine the effects of downburst on structures (e.g., Holmes & Oliver[8]). Rather than relying on the time varying features of one storm, this study employs a half-sine wave to describe this feature representing the transient nature of the storm. In general, it captures the dynamics, if not the exact time variation, of winds in a gust-front. This is defined in this study as

$$V(t) = \sin\left(\frac{\pi}{t_d} t\right) \qquad (3)$$

where, t_d : pulse duration of excitation. In this way, it reasonably describes a single large peak of time-varying mean of a gust-front type wind which is believed to be dominant in structural mo-

tion, and it is a very simple form in which only a single parameter, t_d, is used to define the time function in a gust-front wind. Other pulse shapes, including designer shapes, can be incorporated in this model.

2.3 Profile criteria for comparison between gust-front wind and boundary-layer wind

Strictly speaking, the vertical profile model of a downburst describes short time averaged maximum mean wind speed at a height. Thus, this profile may be regarded as gust profile in the boundary-layer wind sense, not the mean profile. Since z_{max} and V_{max} of the Vicroy model are indeed unknown, it is required to set some criterion to evaluate effects of gust-front winds corresponding to boundary-layer winds and to implement the gust-front factor. For the purpose of practical consideration, two criteria are assumed: First, gust-front wind speed at 10 m height ($V_{G-F}(10)$) is set equal to boundary-layer gust speed at 10 m ($V_{B-L}(10)$); Second, the maximum gust-front wind speed (V_{max}) is equal to gust speed at the gradient height ($V_{B-L}(z_G)$) of boundary-layer wind. The two criteria are expressed in the following expressions; Criterion 1 : $V_{G-F}(10) = V_{B-L}(10)$ and Criterion 2 : $V_{max} = V_{B-L}(10)$.

2.4 Consideration of terrain exposure conditions (terrain roughness)

Although the vertical model chosen above is in reality an analytical/empirical model based on the limited full-scale data, JAWS, which represents one terrain exposure condition, e.g., airport area , it may be regarded as Exposure C in ASCE 7. Thus, it is expected that there is a certain terrain roughness effect on both z_{max} and V_{max} in the Vicroy model, i.e., these two parameters may change with exposure categories in ASCE 7 (Exposure B, C and D in ASCE 7-05 and Exposure A, B, C and D in ASCE 7-98), whereas the model constants b_1 and b_2 (2) are assumed to be constants irrespective of the terrain roughness. Even though this terrain roughness effect on z_{max} and V_{max} has been observed by some researchers through wind-tunnel experiments, the results have been limited to show variation trends on different terrain roughness and were not quantified. Then general trends based on the experimental results showed that the rougher terrain exhibited the higher z_{max} (e.g., Hangan & Xu[9]) and lower V_{max} (e.g., Wood et al.[10]; Choi[11]). In this study, z_{max} is assumed to follow the expression.

$$\frac{z_{max}}{z^*} = \frac{z_{max,z_G}}{z_{G,C}} \qquad (4)$$

where, z^* : a height where half maximum wind velocity occurs, $z_{max,ZG}$: z_{max} obtained from gradient height (z_G) of each terrain exposure condition and $z_{G,C}$: gradient height in the Exposure C of about 274 m (900 ft) in ASCE 7. Then, the modified ratios of z_{max}/z^* considering arbitrary terrain exposure condition become 0.37, 0.29, 0.22 and 0.12 from Exposure A to D, respectively.

Similar to the procedure used in the estimation of z_{max} to account for several terrain exposures, the underlying V_{max} is assumed to be the velocity in Exposure C, and then variation in V_{max} for arbitrary terrain exposure condition is assumed to follow the same relationship of the respective terrain velocity to that of the boundary-layer wind in Exposure C. By using two profile criteria, i.e., Criterion 1 and 2 as mentioned earlier, first $V_{max,C}$ (V_{max} in the Exposure C) which will be the reference value for the consideration of any arbitrary terrain exposure condition can be obtained.

$$\text{Criterion 1}: V_{max,C} = \frac{V_{3-s}}{1.354\left[e^{b_1 10/z_{max,C}} - e^{b_2 10/z_{max,C}}\right]} \qquad (5a)$$

$$\text{Criterion 2}: V_{max,C} \approx 1.42 V_{3-s} \qquad (5b)$$

Here, velocity factor (V_{fac}) is introduced to account for various terrain exposure conditions in V_{max}. To determine V_{fac}, it is assumed that the factor is obtained from the ratio of boundary-layer wind speed at z_{max} of arbitrary terrain exposure condition and boundary-layer wind speed at z_{max} in Exposure C. For example, the velocity factor V_{fac} in the Exposure A condition can be obtained from above assumption.

$$V_{fac} = \frac{\hat{b}_{A-D}}{\hat{b}_C} \cdot \left(\frac{z_{max,A-D}}{10}\right)^{\hat{\alpha}_{A-D} - \hat{\alpha}_C} \qquad (6)$$

where, subscript C : Exposure C condition, subscript A-D : arbitrary exposure condition from A to D (ASCE 7-98). As a result, V_{max} for an arbitrary terrain exposure condition can be obtained from following equation.

$$V_{max} = V_{fac} \cdot V_{max,C} \qquad (7)$$

By using this new definition of V_{max} to account for an arbitrary terrain exposure condition, the vertical profile of gust-front wind can be finally determined from Eq. (2).

Table 1 shows values of V_{max} and z_{max} for other terrains by assuming V_{3-s} as 40 m/s. These results follow the trends noted in experimental observations, i.e., as terrain roughness increases, V_{max} decreases but z_{max} increases. In addition, the criterion of a $V_{G-F}(10) = V_{B-L}(10)$ has a much larger V_{max} than that of $V_{max} = V_{B-L}(z_G)$, and it is because $V_{G-F}(z)$ has a very low wind speed below z_{max}.

It is very important to emphasize here that the models adopted in this section are for the sake of establishing an analysis framework. As additional models become available, those can be incorporated in this framework conveniently.

3 GUST-FRONT FACTOR

With the exemplary success of the gust loading factor in capturing the dynamic wind effects introduced by buffeting and its popularity in design standards and codes, the authors were encouraged to formulate an enhanced framework based on the existing ASCE gust effect formulation that encapsulates the critical features of downburst winds to capture their attendant dynamic load effects. The design load in a gust-front is expressed by

$$F_{Design} = F_{ASCE7} \cdot factor \qquad (8)$$

where F_{Design} is the design load in gust-front wind, F_{ASCE7} is the current recommendation of ASCE 7 (ASCE[5]) and *factor* is the factor that relates F_{Design} to F_{ASCE7}.

In general, the conventional gust loading factor is obtained from displacement relationship, i.e., a ratio of maximum displacement over mean displacement of a structure subject to wind load (Davenport[1]). By means of stationary wind model, the conventional gust loading factor can be denoted by its definition as follows.

$$G_{GLF} = \frac{\max[x_{B-L}(z,t)]}{\text{mean}[x_{B-L}(z,t)]} = \frac{\hat{x}_{B-L}(z,t)}{\overline{x}_{B-L}(z)} \qquad (9)$$

where, subscript B-L : abbreviation of boundary-layer wind, $x_{B-L}(z,t)$: total displacement, $\overline{x}_{B-L}(z)$: mean displacement by mean wind load.

Different from boundary-layer winds, gust-front winds may be regarded as nonstationary due to their transient characteristics. In other words, a stationary wind model used in the boundary-layer wind may not be valid for the gust-front wind which may be described in terms of time-varying parameters. Thus, it is required to introduce a nonstationary wind model as follows (Wang & Kareem[2]).

$$U_{G-F}(z,t) = V_{G-F}(z,t) + u_{G-F}(z,t) \qquad (10)$$

where, subscript G-F : abbreviation of gust-front wind, $V_{G-F}(t)$: time-varying mean component of gust-front wind and $u_{G-F}(z,t)$: fluctuating component of gust-front wind. Then, structural displacement by gust-front winds can also be described as a nonstationary model:

$$x_{G-F}(z,t) = \bar{x}_{G-F}(z,t) + \tilde{x}_{G-F}(z,t) \qquad (11)$$

where, $x_{G-F}(z,t)$: total displacement by gust-front wind, $\bar{x}_{G-F}(z,t)$: displacement by time-varying mean component and $\tilde{x}_{G-F}(z,t)$: displacement by fluctuating component of wind. Its maximum displacement can be expressed by

$$\max\left[x_{G-F}(z,t)\right] = \max\left[\bar{x}_{G-F}(z,t)\right] + \max\left[\tilde{x}_{G-F}(z,t)\right]$$
$$= \max\left[\bar{x}_{G-F}(z,t)\right]\left[1 + \frac{\max\left[\tilde{x}_{G-F}(z,t)\right]}{\max\left[\bar{x}_{G-F}(z,t)\right]}\right] \qquad (12)$$

In addition, $\max[\bar{x}_{G-F}(z,t)]$ can be rewritten by means of its static displacement, $\bar{x}_{st,G-F}(z)$, since the time-varying mean component still has dynamic characteristics unlike the mean displacement of boundary-layer wind.

$$\max\left[\bar{x}_{G-F}(z,t)\right] = \bar{x}_{st,G-F}(z) \cdot \frac{\max\left[\bar{x}_{G-F}(z,t)\right]}{\bar{x}_{st,G-F}(z)} \qquad (13)$$

As mentioned earlier, the *factor* in Eq. (8) describes the relationship between F_{Design} and $F_{ASCE\ 7}$. Similar to the gust loading factor (G_{GLF}) concept which is obtained from a displacement relationship (9), the *factor* is defined as a ratio of maximum displacements between gust-front winds and boundary-layer winds in this study. By using Eqs. (9) to (13), the *factor* in Eq. (8) can be rewritten by

$$factor = \frac{\max\left[x_{G-F}(z,t)\right]}{\max\left[x_{B-F}(z,t)\right]} = \frac{\bar{x}_{st,G-F}(z) \cdot \dfrac{\max\left[\bar{x}_{G-F}(z,t)\right]}{\bar{x}_{st,G-F}(z)} \cdot \left[1 + \dfrac{\max\left[\tilde{x}_{G-F}(z,t)\right]}{\max\left[\bar{x}_{G-F}(z,t)\right]}\right]}{\bar{x}_{B-L}(z) \cdot G_{GLF}} \qquad (14)$$

Here, variable y is introduced which is a displacement without consideration of the drag force coefficient since gust-front winds may have transient characteristics and it may yield a different aerodynamic drag force coefficient on structures, i.e., transient drag force coefficient ($C_{D,G-F}$). By separating the drag force coefficient, x in Eq. (14) is replaced by y for displacement in gust-front and boundary-layer winds. This recasts Eq. (14) as

$$factor = \frac{\bar{y}_{st,G-F}(z)}{\bar{y}_{B-L}(z)} \cdot \frac{\max\left[\bar{y}_{G-F}(z,t)\right]}{\bar{y}_{st,G-F}(z)} \cdot \frac{\left[1 + \dfrac{\max\left[\tilde{y}_{G-F}(z,t)\right]}{\max\left[\bar{y}_{G-F}(z,t)\right]}\right]}{G_{GLF}} \cdot \frac{C_{D,G-F}}{C_D} \qquad (15)$$

A "Gust-Front Factor" (G_{G-F}) is introduced for use in conjunction with the existing design codes and standards. Based on Eq. (15), the design load in gust-front wind (8) is described as

$$F_{Design} = F_{ASCE\ 7} \cdot K_{z,G-F} \cdot G_{G-F} \qquad (16)$$

$$K_{z,G-F} = \frac{\bar{y}_{st,G-F}(z)}{\bar{y}_{B-L}(z)} \qquad (17)$$

where, $K_{z,G-F}$ is the velocity pressure coefficient that is similar to the current ASCE 7 for boundary-layer winds used to account for the velocity/pressure profile in a gust-front (17) and G_{G-F} is the gust-front factor.

Gust-front factor (G_{G-F}) consists of three underlying factors as given below (Kareem et al.[5]).

$$G_{G-F} = I_1 \cdot I_2 \cdot I_3 \qquad (18)$$

where,

$$I_1 = \frac{\max\left[\bar{y}_{G-F}(z,t)\right]}{\bar{y}_{st,G-F}(z)}; \quad I_2 = \frac{\left[1 + \dfrac{\max\left[\tilde{y}_{G-F}(z,t)\right]}{\max\left[\bar{y}_{G-F}(z,t)\right]}\right]}{G_{GLF}}; \quad I_3 = \frac{C_{D,G-F}}{C_D} \qquad (19)$$

where, G_{GLF} and C_D : gust loading factor and drag force coefficient in boundary-layer wind, respectively. In this manner, G_{G-F} takes into consideration the following dynamic features: dynamics effects introduced by the sudden rise in wind speed - pulse dynamics factor (rise-time effects), I_1; nonstationarity of turbulence in gust-front wind - structural dynamics factor (nonstationary turbulence effects), I_2; transient aerodynamics - load modification factor (transient aerodynamics effects), I_3. By separating the G_{G-F} into three major features, it offers an intuitive picture of the underlying mechanisms attendant to the load effects of gust-front winds on structures. A schematic diagram portraying the anatomy of the design wind loads in gust-fronts is given in Figure 1.

4 EXAMPLE

An example building is used to evaluate the G_{G-F}: building width and depth = 40 m; building height = 200 m; natural frequency = 0.2 Hz;, building bulk density = 180 kg/m³; air density = 1.25 kg/m³; damping ratio = 0.01; z_{max} = 60 m; V_{max} = 57 m/s ; Criterion 2 (Eq. 4b) in vertical profile condition; pulse duration t_d = 200 sec. I_3 is assumed to be unity in this study since this is a subject of current research.

Based on the building dynamic parameters, it is noted that factor I_1 is unity, which points at the lack of pulse dynamic effect for this particular building. Moreover, factor I_2 turns out to be less than unity and it means that nonstationary turbulence effects of gust-front winds may not be significant in this case and due to short duration of the event the peak response may not have attained values comparable to stationary cases. A similar observation was noted in Chay & Albermani[12]. Finally, gust-front factor of 0.82 is obtained from a product of I_1, I_2 and I_3 as shown in Table 2. G_{G-F} of less than unity suggests that dynamic effects introduced on the example building in the modeled gust-front winds are less significant than those in conventional boundary-layer winds.

Figure 2 shows design loads in a gust-front utilizing Eq. (16). It is noted that despite the insignificance of the dynamic effects contributed by the pulse dynamics and nonstationary aspects (Fig. 1) the static effects due to the wind profile result in locally accentuated loads around z_{max}.

This underscores the role of enhancement in the static effects introduced through the velocity pressure coefficient ($K_{z,G-F}$) to the overall design load even though the dynamic effects were not significant for this particular example. One should not overlook the possible load enhancement due to transient aerodynamics (Fig. 1), which may be attributed to the changes in the aerodynamics associated with the fast moving front around the building with better spatial correlation of the flow field.

5 CONCLUDING REMARKS

Winds associated with gust-fronts is an emerging issue in the field of wind/structural engineering due to their nonstationary characteristics and their capacity to inflict significant damage on structures. Design wind loads based on conventional analysis frameworks in codes and standards may not accurately describe this fundamentally different wind event that departs from typical boundary-layer winds both in its kinematics and dynamics. This paper proposes a gust-front factor approach that accounts for the changes in load effects in gust-front winds and can be used in conjunction with the existing design standards. The conventional gust loading factor approach becomes a special case of the proposed scheme as in the case of G_{G-F} and $K_{z,G-F}$, reducing to unity in Eq. (16). In the example studied here, it is observed that higher local loading in the ESWL distribution on the building exists even though the G_{G-F} is less than unity. The proposed gust-front factor based analysis framework lays the foundation for the analysis of structures under gust-front winds, which is akin to the gust loading factor in conventional winds. It can conveniently tailored for design standards other than ASCE 7. It is anticipated that it would experience further refinements over time similar to the many subsequent developments in the conventional gust loading factor. For immediate design applications, this framework is available in a web-based portal which will offer the flexibility of studying several loading configurations without actually becoming involved with the details of the computations, making it independent of the technical background of the user. It has a user-friendly interface which is shown in Figure 3 and available at http://gff.ce.nd.edu.
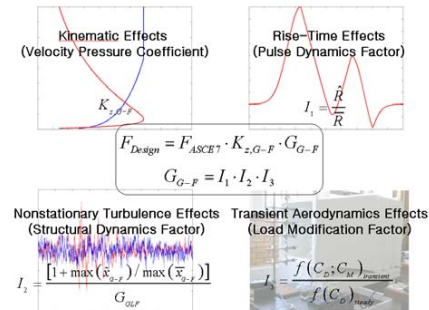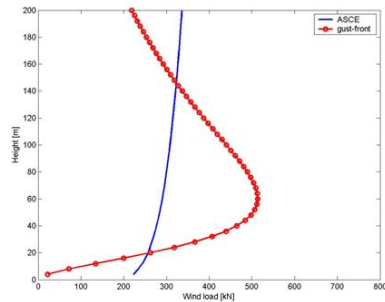
7 REFERENCES

1 A. G. Davenport, Gust loading factors, Journal of the Structural Division, ASCE, 93(3) (1967) 11-34.
2. A. Kareem and Y. Zhou, Gust loading factor - past, present and future, Journal of Wind Engineering and Industrial Aerodynamics, 91(12-15) (2003) 1301-1328.
3. L. Wang and A. Kareem, Modeling of non-stationary winds in gust-fronts, Proc. of 9th ASCE Joint Specialty Conference on Probabilistic Mechanics and Structural Reliability, PMC2004, Albuquerque, New Mexico, 2004.
4. L. Chen and C. W. Letchford, Parametric study on the along-wind response of the CAARC building to downbursts in the time domain, Journal of Wind Engineering and Industrial Aerodynamics, 92 (2004) 703-724.
5 ASCE 7-98, 7-05, Minimum design loads for buildings and other structures, American Society of Civil Engineers.
6. A. Kareem, K. Butler, and D. Kwon, Modeling and simulation of transient wind load effects, Proc. of the 4th UJNR Panel on Wind and Seismic Effects Workshop on Wind Engineering, Tsukuba, Tokyo (2006).
7 D. D. Vicroy, A simple, analytical, axisymmetric microburst model for downdraft estimation, NASA Technical Memorandum, 104053, 1991.
8 J. D. Holmes, J. D and S. E. Oliver, An empirical model of a downburst, Engineering Structures, 22 (2000) 1167-1172.
9 H. Hangan and Z. Xu, Scale and roughness effects in impinging jets with application to downburst simulations, Proceedings of 10th Americas Conference on Wind Engineering, Baton Rouge, Louisiana (2005).
10 G. S. Wood, K. C. S. Kwok, N. A. Motteram and D. F. Fletcher, Physical and numerical modelling of thunderstorm downbursts, Journal of Wind Engineering and Industrial Aerodynamics 89 (2001) 535-552.
11 E. C. C. Choi, Field measurement and experimental study of wind speed profile during thunderstorms, Journal of Wind Engineering and Industrial Aerodynamics, 92 (2004) 275-290.
12 M. Chay, and F. Albermani, Dynamic Response of a SDOF system subjected to simulated downburst winds, Proceedings of the Sixth Asia-Pacific Conference on Wind Engineering (APCWE-VI), Seoul, Korea (2005).
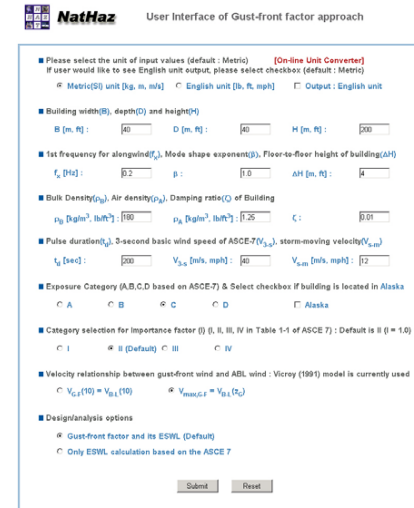
Figure 3. User-friendly interface of web-based on-line gust-front factor approach

Table 1. V_{max} and z_{max} for terrain exposure condition (V_{3-s} is assumed as 40 m/s)

	V_{max} (m/s)		z_{max} (m)
	Criterion 1	Criterion 2	
Exp. A	71.26	45.15	100.58
Exp. B	81.29	51.50	80.47
Exp. C	89.47	56.68	60.35
Exp. D	93.06	58.96	46.94

Table 2. Gust-front factor and its sub-factors

I_1	I_2	I_3	G_{G-F}
1.00	0.82	1.00	0.82

Figure 1. Schematic diagram of gust-front factor and its sub-factors (Kareem et al.[5])

Figure 2. ESWL in ASCE 7 and gust-front wind